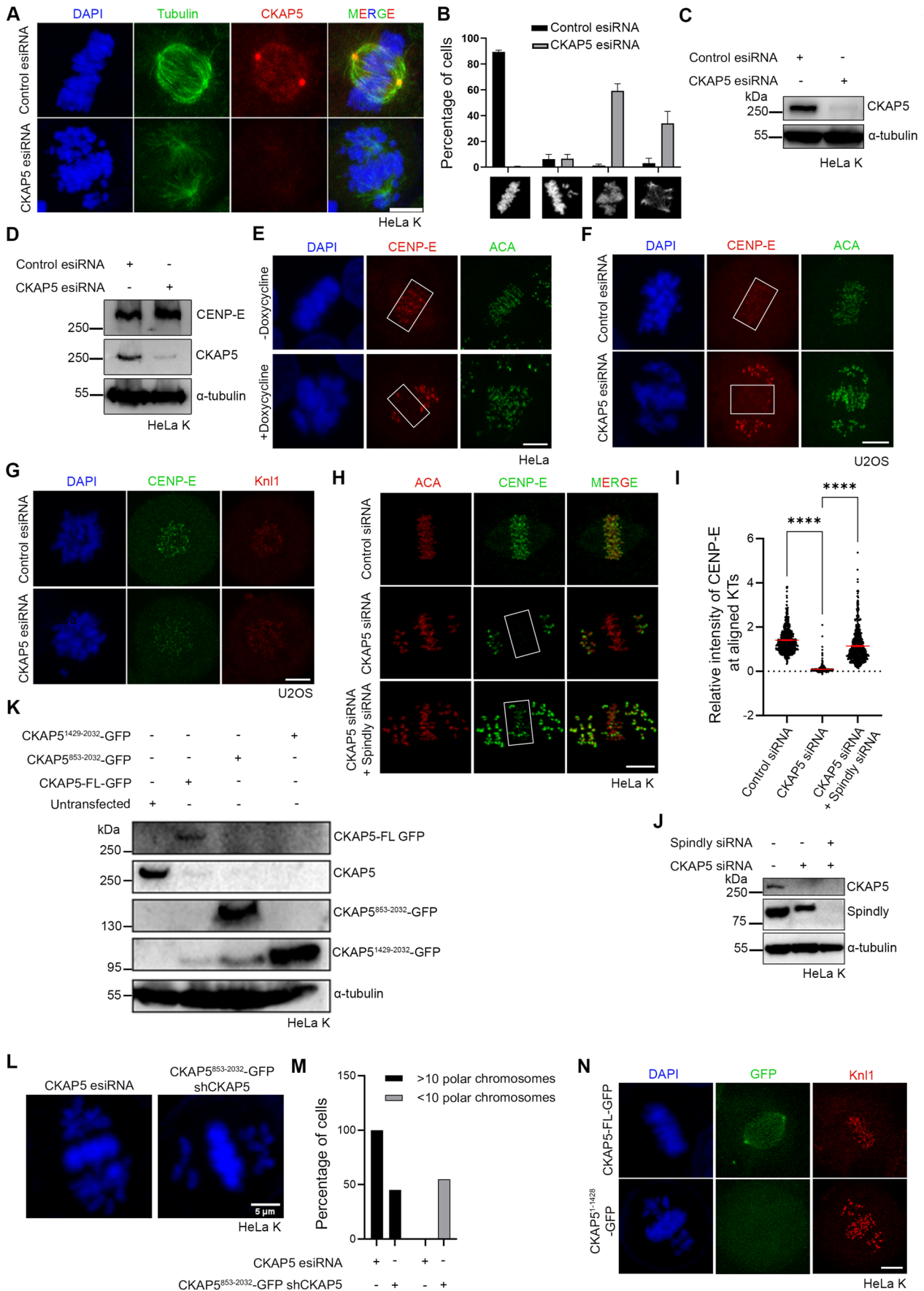
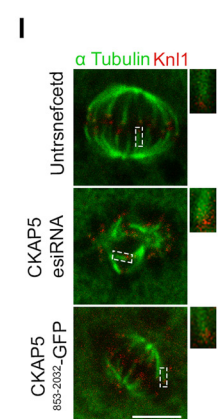
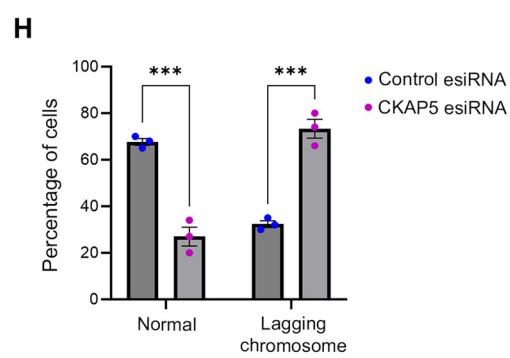
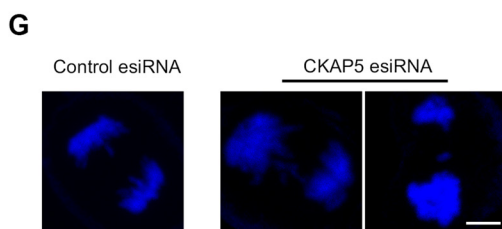
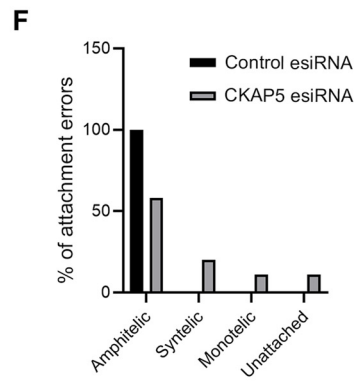
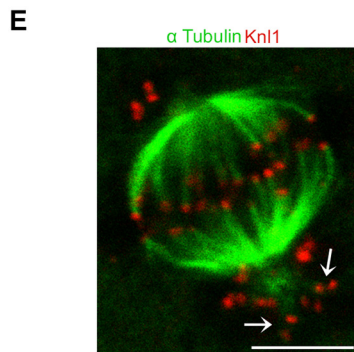
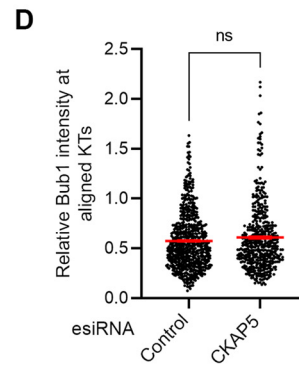
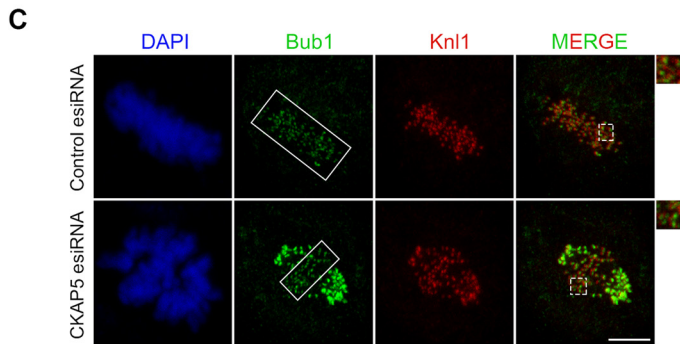
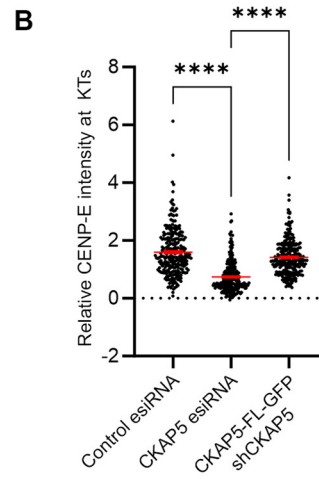
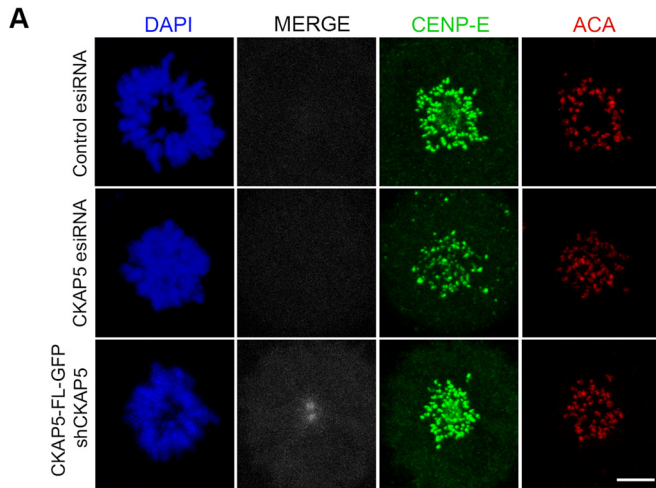


Expanded View Figures

Figure EV1. CKAP5 depletion induces chromosome misalignment and removal of CENP-E from kinetochores.

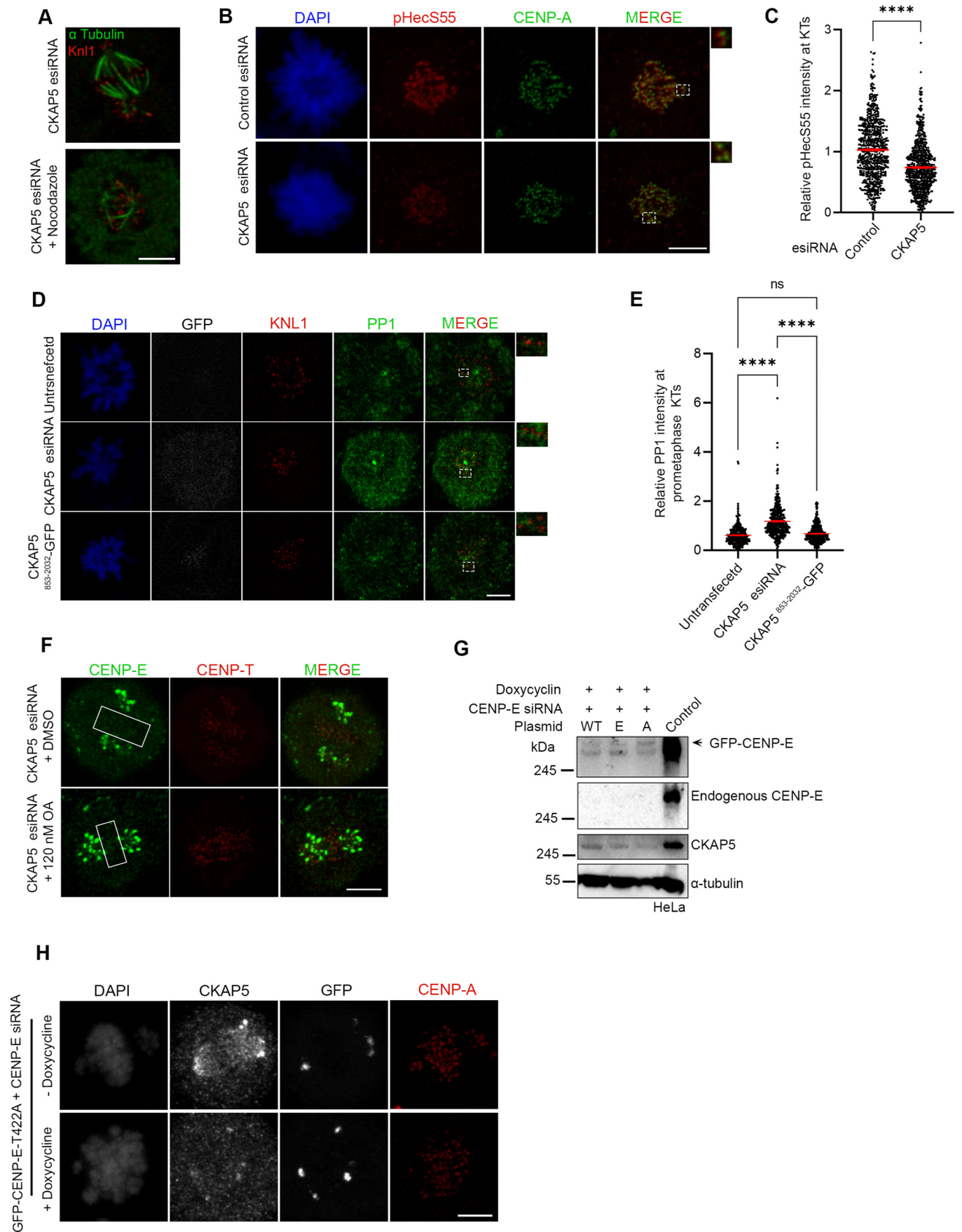
(A) Representative immunofluorescence images showing level of CKAP5 depletion and chromosome misalignment phenotype. (B) Quantification of chromosome misalignment phenotypes ($n > 100$ cells in each case) in CKAP5-depleted cells compared to mock-treated (control esiRNA) cells from three independent experiments. Data represents mean \pm SEM. (C, D) Western blots showing level of CKAP5 depletion and corresponding cellular levels of CENP-E. (E) Representative immunofluorescence images showing removal of CENP-E from partially aligned KTs of inducible Cas-9 expressing CKAP5 knockout HeLa cells (regions shown in box). (F, G) Immunofluorescence images showing loss of CENP-E localization at the partially aligned metaphase KTs (regions shown in box) and prometaphase KTs of U2OS cells depleted of endogenous CKAP5. (H) Representative immunofluorescence images showing rescue of CENP-E localization at aligned KTs in CKAP5-Spindly co-depleted HeLa Kyoto cells compared to control metaphase and CKAP5-depleted cells (regions shown in box). (I) Dot plot showing mean intensity of endogenous CENP-E at aligned KTs (highlighted with boxes) normalized with that of ACA where each dot represents individual KT ($n = 400$ -550) quantified from multiple cells from three independent experiments. **** $P < 0.0001$ by one-way ANOVA. Data represents mean \pm SEM. (J) Western blot showing levels of CKAP5 and Spindly depletion in HeLa Kyoto cells. (K) Western blot showing endogenous CKAP5 depletion levels in the cells expressing GFP-tagged CKAP5-FL vs. different deletion constructs. (L) Immunofluorescence images showing chromosome phenotype in CKAP5-depleted cells (HeLa Kyoto) and in cells expressing fusion construct consisting of CKAP5⁸⁵³⁻²⁰³²-GFP and CKAP5-shRNA. (M) Plot showing percentage of cells ($n = 73$ cells) with less than 10 polar chromosomes in CKAP5⁸⁵³⁻²⁰³²-GFP-CKAP5-shRNA cells compared to CKAP5 esiRNA-treated cells (HeLa Kyoto). (N) Representative immunofluorescence image of HeLa Kyoto cell expressing CKAP5¹⁻¹⁴²⁹-GFP in endogenous CKAP5-depleted background showing no recognizable KT or spindle localization. Scale bar of all images = 5 μ m. Data Information: Chromosome congression defect and level of CKAP5 depletion (red) by immunofluorescence imaging (A). Rectangular boxes show aligned KTs with normal CENP-E localization in control vs. reduced CENP-E localization in CKAP5-depleted conditions (E, F). Doxycycline-inducible CKAP5 KO HeLa cells in (E) and U2OS cells in (F). CKAP5-depleted cells shows reduced CENP-E levels (green) at KTs compared to control cells when arrested in prometaphase by Eg5 kinesin inhibition (G). Rectangular boxes show region (aligned KTs) considered for CENP-E intensity analysis. Rescue in CENP-E levels (green) are observed upon co-depletion of spindly and CKAP5 (H). DAPI staining of chromosomes showing reduction in number of polar chromosomes upon expression of CKAP5⁸⁵³⁻²⁰³²-GFP compared to that in CKAP5-depleted condition (L). CKAP5¹⁻¹⁴²⁹-GFP (green) showing no localization in HeLa Kyoto cells when compared to CKAP5-FL-GFP (green) under endogenous CKAP5-depleted condition (N).





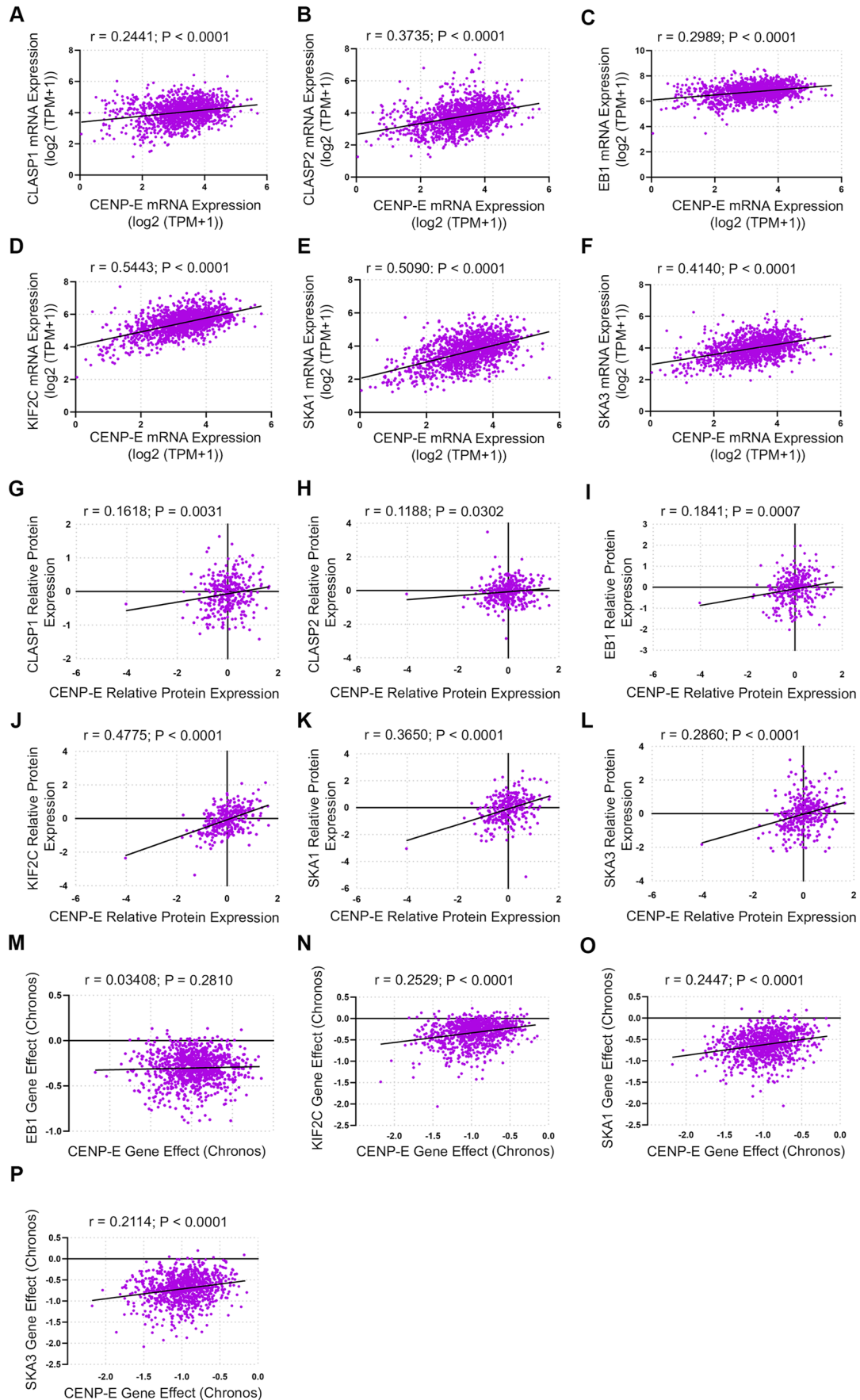
◀ **Figure EV2. CKAP5 depletion results in kinetochore-microtubule attachment errors and lagging chromosomes.**

(A) Representative immunofluorescence images showing rescue of CENP-E (green) localization at prometaphase KT of HeLa Kyoto cells expressing CKAP5-FL-GFP (grey) when compared to CKAP5-depleted cells. ACA (red) was used as KT marker. (B) Dot plot showing mean intensity of endogenous CENP-E at these KT normalized with that of ACA where each dot represents individual KT ($n = 270$) quantified from multiple cells from three independent experiments. **** $P < 0.0001$ by one-way ANOVA. (C) Representative immunofluorescence image showing no significant change in localization of Bub1 at aligned KT of control vs. CKAP5-depleted HeLa Kyoto cells. Insets show enlarged view of region marked by dotted boxes in the merge images. (D) Dot plots showing mean intensities of Bub1/Knl1 ($n = 400$ KT) quantified from individual kinetochores of multiple cells from three independent experiments. (E) Representative immunofluorescence image showing syntelic attachments (marked with arrowheads) of polar chromosomes. (F) Plot showing percentage of amphitelic, syntelic, monotelic and unattached KT (144 KT pairs from multiple cells) of pole-proximal chromosomes in CKAP5-depleted HeLa Kyoto cells. (G) Anaphase lagging chromosomes shown by CKAP5-depleted HeLa Kyoto cells. (H) Graph showing increased percentage of cells showing anaphase laggards upon depletion of CKAP5. More than 100 cells were analyzed from three independent experiments. *** $P = 0.0007$ by two-way ANOVA. (I) Representative immunofluorescence images (single plane) showing cold stable microtubule staining (α Tubulin in green; KNL1 in red) in HeLa Kyoto cells expressing CKAP5 esiRNA and CKAP5⁸⁵³⁻²⁰³²-GFP compared to un-transfected HeLa Kyoto cells. Region in dashed boxes is enlarged in inset. Scale bar of all images = 5 μ m. All data represents mean \pm SEM. Data Information: Expression of CKAP5-FL-GFP (grey) rescued CENP-E levels (green) at prometaphase KT under endogenous CKAP5-depleted condition (A). Rectangular boxes show region (aligned KT) taken for Bub1 intensity analysis. Dotted boxes in merged images showing few KT enlarged in inset. Bub1 (green) levels showed no difference (C). Arrows show KT of polar chromosomes with syntelic attachments (E). DAPI staining of anaphase chromosomes of control and CKAP5-depleted cells. CKAP5-depleted cells showed multiple lagging chromosomes (G). Dotted rectangular boxes are enlarged in insets showing increased MT (green) thickness in CKAP5-depleted condition and rescued MT intensity upon expression of CKAP5⁸⁵³⁻²⁰³²-GFP (I).



◀ **Figure EV3. CKAP5 depletion leads to increased PP1 activity at the partially aligned kinetochores.**

(A) Representative immunofluorescence image showing partial destabilization of MTs in CKAP5-depleted HeLa Kyoto cells using 3.3 μ M nocodazole for 10 min. (α Tubulin in green; KNL1 in red). (B) Immunofluorescence images showing pHecS55 (red) and CENP-A (green) at prometaphase kinetochores of control and CKAP5-depleted HeLa Kyoto cells. Insets show the enlarged view of the dashed boxes. (C) Dot plot showing mean fluorescence intensity of pHecS55 normalized to that of CENP-A quantified from individual kinetochores ($n \sim 700$ KTs) of multiple cells from three independent experiments. **** $P < 0.0001$ by Student's t test. (D) Immunofluorescence images (single plane) showing PP1 (green) and KNL1 (red) at prometaphase KTs of HeLa Kyoto cells expressing CKAP5 esiRNA and CKAP5⁸⁵³⁻²⁰³²-GFP compared to un-transfected cells. Regions in dashed boxes are enlarged in insets. (E) Dot plot showing mean fluorescence intensity of PP1 from individual kinetochores ($n \sim 400$ KTs) normalized with that of KNL1. KTs from individual z planes of multiple cells were analyzed from three independent experiments. **** $P < 0.0001$ by one-way ANOVA. (F) Representative immunofluorescence image showing localization of CENP-E in CKAP5 esiRNA-treated cells incubated with DMSO or 120 nM okadaic acid. Boxes show region of aligned KTs. (G) Western blot showing endogenous CENP-E depletion and doxycycline-induced depletion of CKAP5 in doxycycline-inducible CKAP5 KO HeLa. (WT-Wildtype; A-T422A; E- T422E). (H) Representative immunofluorescence images showing KT localization of GFP-CENP-E-T422A in the presence or absence of doxycycline in doxycycline-inducible CKAP5 KO HeLa cells under endogenous CENP-E depleted background. All data represent mean \pm SEM. Scale bar of all images = 5 μ m. Data Information: MTs (green) show partial destabilization upon treatment with 3.3 μ M nocodazole for 10 min (A). Dotted boxes in merged image are enlarged in insets showing increased levels of pHecS55 (red) at prometaphase KTs upon CKAP5 depletion (B). Dotted boxes in merged image show few KTs that are enlarged in insets. PP1 levels (green) at prometaphase KTs were rescued upon expression of CKAP5⁸⁵³⁻²⁰³²-GFP (D). Rectangular boxes show level of CENP-E (green) at aligned KTs. No change in CENP-E levels were observed upon treatment with low concentration of okadaic acid to inhibit PP2A (F). GFP-CENP-E-T422A showed no localization to aligned KTs in the presence or absence of CKAP5 (H).



◀ Figure EV4. Correlation between CKAP5 and CENP-E with respect to other spindle/kinetochore proteins.

(A–F) Correlation of mRNA expression of CENP-E and multiple spindle/kinetochore proteins. (A) CLASP1, (B) CLASP2, (C) EB1, (D) KIF2C, (E) SKA1, (F) SKA3. The correlation is similar across proteins and similar to the correlation between CKAP5 and CENP-E mRNA expression (Fig. 6E). (G–L) Correlation of protein expression of CENP-E and multiple spindle/kinetochore proteins—(G) CLASP1, (H) CLASP2, (I) EB1, (J) KIF2C, (K) SKA1, (L) SKA3. The correlation is similar across proteins and similar to the correlation between CKAP5 and CENP-E protein expression (Fig. 6F). (M–P) Correlation of sensitivity to CRISPR gene perturbation of CENP-E and multiple spindle/kinetochore proteins. All data is normalized to the mRNA expression of the proliferation marker MKI67 as a covariate using a linear model. (M) EB1, (N) KIF2C, (O) SKA1, (P) SKA3. The correlation is similar across proteins and to the correlation between CKAP5 and CENP-E CRISPR perturbation sensitivity (Fig. 6G). All data is normalized to the mRNA expression of the proliferation marker MKI67 as a covariate using a linear model. Two-sided Pearson's correlation was used for all the data analysis.